NASA/TM—2019–220072

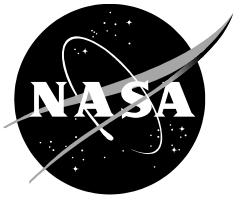

Urban Air Mobility Network and Vehicle Type—Modeling and Assessment

Lee W. Kohlman
Ames Research Center, Moffett Field, California

Michael D. Patterson
Langley Research Center, Hampton, Virginia

Brooke E. Raabe
University of California Davis, Davis, California

February 2019

NASA STI Program ... in Profile

Since its founding, NASA has been dedicated to the advancement of aeronautics and space science. The NASA scientific and technical information (STI) program plays a key part in helping NASA maintain this important role.

The NASA STI program operates under the auspices of the Agency Chief Information Officer. It collects, organizes, provides for archiving, and disseminates NASA's STI. The NASA STI program provides access to the NTRS Registered and its public interface, the NASA Technical Reports Server, thus providing one of the largest collections of aeronautical and space science STI in the world. Results are published in both non-NASA channels and by NASA in the NASA STI Report Series, which includes the following report types:

- TECHNICAL PUBLICATION. Reports of completed research or a major significant phase of research that present the results of NASA Programs and include extensive data or theoretical analysis. Includes compilations of significant scientific and technical data and information deemed to be of continuing reference value. NASA counterpart of peer-reviewed formal professional papers but has less stringent limitations on manuscript length and extent of graphic presentations.

- TECHNICAL MEMORANDUM. Scientific and technical findings that are preliminary or of specialized interest, e.g., quick release reports, working papers, and bibliographies that contain minimal annotation. Does not contain extensive analysis.

- CONTRACTOR REPORT. Scientific and technical findings by NASA-sponsored contractors and grantees.

- CONFERENCE PUBLICATION. Collected papers from scientific and technical conferences, symposia, seminars, or other meetings sponsored or co-sponsored by NASA.

- SPECIAL PUBLICATION. Scientific, technical, or historical information from NASA programs, projects, and missions, often concerned with subjects having substantial public interest.

- TECHNICAL TRANSLATION. English-language translations of foreign scientific and technical material pertinent to NASA's mission.

Specialized services also include organizing and publishing research results, distributing specialized research announcements and feeds, providing information desk and personal search support, and enabling data exchange services.

For more information about the NASA STI program, see the following:

- Access the NASA STI program home page at http://www.sti.nasa.gov

- E-mail your question to help@sti.nasa.gov

- Phone the NASA STI Information Desk at 757-864-9658

- Write to:
  NASA STI Information Desk
  Mail Stop 148
  NASA Langley Research Center
  Hampton, VA 23681-2199

NASA/TM—2019–220072

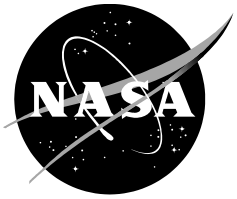

Urban Air Mobility Network and Vehicle Type—Modeling and Assessment

Lee W. Kohlman
Ames Research Center, Moffett Field, California

Michael D. Patterson
Langley Research Center, Hampton, Virginia

Brooke E. Raabe
University of California Davis, Davis, California

National Aeronautics and
Space Administration

Ames Research Center
Moffett Field, CA 94035-1000

February 2019

ACKNOWLEDGMENTS

This work was funded by the NASA Aeronautics Research Mission Directorate under the Revolutionary Vertical Lift Technologies Project of the Advanced Air Vehicles Program and the Convergent Aeronautics Solutions Project of the Transformational Aeronautics Concepts Program.

Available from:

NASA STI Support Services
Mail Stop 148
NASA Langley Research Center
Hampton, VA 23681-2199
757-864-9658

National Technical Information Service
5301 Shawnee Road
Alexandria, VA 22312
info@ntis.gov
703-605-6000

This report is also available in electronic form at
http://ntrs.nasa.gov/

TABLE OF CONTENTS

TABLE OF CONTENTS (continued)

LIST OF FIGURES

LIST OF TABLES

NOMENCLATURE

ALF	average load factor
CNG	compressed natural gas
CO_2	carbon dioxide
DEP	distributed electric propulsion
DOC	direct operating cost
GPS	global positioning system
IC	internal combustion
LNG	liquefied natural gas
MJ	megajoules
MTOW	maximum takeoff weight
pax	passengers
SOFC	solid oxide fuel cells
ToL	takeoff and landing
UAM	urban air mobility
VTOL	vertical takeoff and landing

Urban Air Mobility Network and Vehicle Type—Modeling and Assessment

Lee W. Kohlman, Michael D. Patterson,[*] and Brooke E. Raabe[†]

Ames Research Center

SUMMARY

This paper describes exploratory modeling of an on-demand urban air mobility (UAM) network and sizing of vehicles to operate within that network. UAM seeks to improve the movement of goods and people around a metropolitan area by utilizing the airspace for transport. Aircraft sizing and overall network performance results are presented that include comparisons of battery-electric and various hybrid-electric vehicles fueled with diesel, jet fuel, compressed natural gas (CNG), and liquefied natural gas (LNG). Hybrid-electric propulsion systems consisting of internal combustion engine–generators, turbine-generators, and solid oxide fuel cells are explored. Ultimately, the "performance" of the UAM network over a day for each of the different vehicle types, propulsion systems, and stored energy sources is described in four parameters: 1) the average cost per seat-kilometer, which considers the costs of the energy/fuel, vehicle acquisition, insurance, maintenance, pilot, and battery replacement; 2) carbon dioxide emission rates associated with vehicle operations; 3) the average passenger wait time; and 4) the average load factor, i.e., the total number of seats filled with paying passengers divided by the total number of available seats. Results indicate that the "dispatch model," which determines when and where aircraft are flown around the UAM network, is critical in determining the overall network performance. This is due to the often-conflicting desires to allow passengers to depart with minimal wait time while still maintaining a high load factor to reduce operating costs. Additionally, regardless of the dispatch model, hybrid-electric aircraft powered by internal combustion engines fueled with diesel or LNG are consistently the lowest cost per seat-kilometer. Battery-electric and future technology LNG/solid oxide fuel cell aircraft produce the lowest emissions (assuming the California grid) with LNG-fueled internal combustion engine–powered hybrids producing only slightly more carbon dioxide.

I. INTRODUCTION

Urban air mobility (UAM) is a transportation concept in which people and cargo are moved around metropolitan areas in air vehicles as a part of a multi-modal transportation system. Although it could be argued that limited forms of UAM exist today, such as the helicopter services operated by companies like Blade [1], the concept implied by the term UAM consists of much larger numbers of aircraft transporting considerably more people in more routine transportation than existing services provide. To help describe these novel operations, NASA recently proposed the concept of a UAM Maturity Level, which describes a gradual progression

[*] NASA Langley Research Center, Aeronautics Systems Analysis Branch, Hampton, VA, 23681.
[†] University of California Davis, Davis, CA, 95616.

of UAM operations moving from individual test flights to a truly ubiquitous transportation system that would consist of thousands of aircraft flying simultaneously over a single metropolitan area [2]. Many of the proposed UAM transportation services assume that services will be provided in an on-demand or near-on-demand manner so that they can effectively replace trips that are taken by cars today. Prominent proponents for this novel form of transportation system include Uber [3], [4]; Joby Aviation [5], [6]; Lilium [7]; and Kitty Hawk [8].

There are many important issues that must be addressed before widespread UAM transportation systems can be implemented practically, such as vehicle certification and economic viability. Currently existing, certified vehicles lack many of the characteristics necessary to meet all of the requirements of a successful UAM vehicle, including the need for low noise levels and low operating costs. Many different vehicle configurations have been proposed to address the technical and public acceptability requirements around issues such as safety and emissions.

One of the technologies common to many of the emerging UAM vehicles is electrification of the propulsion systems. Distributed electric propulsion (DEP) is one such technology that can enable more efficient vehicle designs than are practical with conventional mechanical systems. DEP relies on electricity to distribute power to multiple motors, which can drive multiple types of propulsion devices such as propellers, rotors, and ducted fans. One application of DEP is to create a high-lift system on a conventional takeoff and landing (ToL) vehicle, which can enable vehicles with a higher cruise efficiency than with conventional high-lift systems alone [9], [10]. DEP can also enable propellers to be placed at wingtips where they can reduce induced drag or increase propulsive efficiency [11], [12]. When applied specifically to vertical takeoff and landing (VTOL) vehicles, DEP enables practical unconventional vehicle designs that can achieve considerably higher cruise efficiency than feasible with conventional rotorcraft [13], though this cruise efficiency typically comes at the cost of a reduced efficiency in hover. Examples of some of these novel vehicle designs include NASA's GL-10 tilting wing and tail unmanned aerial vehicle [13], [14]; lift-plus-cruise configurations like Kitty Hawk's Cora [8]; and Joby Aviation's S2 and S4 multi-tiltrotor configurations [5], [15].

There are many ways in which electrical power for DEP aircraft can be generated on board. The most suitable means of generating electrical power for UAM aircraft, which are typically proposed in the one- to six-passenger-size class, include batteries, an internal combustion (IC) engine with a generator, a turbine with a generator, and a solid oxide fuel cell (SOFC) system that reforms hydrocarbon fuels. Generally speaking, at the scale of interest, the turbine is the lightest system, but also the least fuel efficient. The IC engine with generator is the next lightest, and more efficient than the turbine. The battery and SOFC systems can be comparable to the combustion-based systems in mass and efficiency depending on the range of the mission [16].[‡] This paper presents a comparative analysis of several combinations of fuels and power sources to provide insight into which of these may be the most appropriate for the novel UAM missions being proposed.

[‡] The efficiency of the battery is often cited as 95 percent, but when taking into account the efficiency of electricity generation, the SOFC system can be very competitive. Because of the high specific energy of fuel, a SOFC system will win on a mass basis for longer missions.

The paper begins with a description of how the aircraft, and the network in which they operate, are modeled. The aircraft sizing method uses a power loading model to define the aircraft missions and first order linear approximations for most component masses. A fleet is then built from the sized aircraft, and the fleet operations for one day are simulated. The network model involves a metropolitan area representation (for this paper, the San Francisco Bay Area), a demand model, and a dispatch model. The demand and dispatch models are critically important to identifying various behaviors of the network and deriving direct operating costs (DOCs) for the network. DOC and CO_2 emissions are estimated for a variety of propulsion system technologies. The effects of sizing mission length and SOFC technology level are also explored.

II. VEHICLE SIZING

To compare different aircraft configuration, propulsion system, and energy storage types, the mission that the aircraft is designed to fly must first be specified. Then, various aircraft can be sized to perform that mission so that the relative comparisons between the aircraft are made in an "apples-to-apples" manner. This section describes the methods used to size vehicles for a given mission and presents comparisons of the various vehicles sized with different propulsion systems.

A. Model Assumptions

Because the work in this paper is an extension of what was previously presented in reference [1], many of the same assumptions are made here. The subsections below provide a quick overview of the assumptions, highlighting those items that differ from reference [1].

1. Vehicle Propulsion System Component Specifications

The engine and turbine sizing models for each vehicle type are described in reference [16]. The specific power of the SOFC system is varied to account for potential improvements to this relatively new technology to determine the sensitivity of the DOC and vehicle maximum takeoff weight (MTOW) to the technology level assumed. Specifically, SOFC specific power is set to 312 W/kg for diesel-fueled variant [17] and 350 W/kg for near-term liquefied natural gas (LNG) because of anticipated weight savings with a simplified fuel reformer. Future advanced LNG/SOFC options are considered at 525 W/kg and 700 W/kg for mid- and long-term technology improvements. The efficiency of electricity production from the lower heating value of the fuel for all SOFC systems is assumed to be 60 percent [17].

The battery model is built on a database of commercially available cells, which each have different specific power and specific energy specifications. For simplicity, and to model projected future increases in battery technology that may be present at the time UAM operations occur, the battery pack is assumed to have the same specifications as the cell-level technology (i.e., there is zero "packaging factor" or "overhead" in going from the cell to the battery pack).[§]

[§] It is acknowledged that the inherent tradeoff in specific energy and specific power modeled by this approach may not reflect the real tradeoffs that would occur with wisely designed battery packs (as cells can be connected in parallel and series in different manners within battery packs to optimize the pack architecture). However, the authors believe that this approach provides a reasonable rough estimate for the high-level exploratory analysis performed in this paper.

Table 1. Vehicle Component Assumptions: Specific Power and Efficiency

Item	Specific Power (kW/kg)	Efficiency
IC Engine	0.0009.*design_power + 1.4887	0.000004.*design_power + 0.3699
Turbine Engine	0.2476.*design_power.^0.4509	0.0641.*design_power.^0.2103
SOFC	0.312, 0.350, 0.525, 0.700	0.60
Battery	Varies with cell	0.95
Generator	16	0.95
Rectifier	40	0.985
Bus	1000	0.998
Inverter	25	0.985
Motor	4	0.95
Auxiliary Power Source	25	0.985
Battery Charge Controller	25	0.985
Liquid Cooling System	6.25	1

This approach implies that the battery-electric aircraft discussed in this paper could not be produced today and relies on technological improvement. The maximum specific energy that can be selected is 293 Wh/kg, which has an associated specific power of 586 W/kg. Additionally, to demonstrate the impact that even further future increases in battery technology may have, results with a "technology factor" of 1.5 applied to the specific energy of the batteries from the database are also shown. This factor has the impact of increasing the maximum specific energy in the database to 440 Wh/kg. Additional assumptions are included in Table 1.

2. Aircraft Sizing Process

The sizing mission is defined by specifying the power loading (i.e., kW/kg) over time. An example power loading mission profile is presented in Figure 1. In this example, the mission begins with a taxi segment, which requires a power loading of 0.0083 kW/kg for 30 seconds. Next, there is a takeoff segment requiring 0.25 kW/kg for 30 seconds followed by a transition segment, which requires 0.2 kW/kg for 30 seconds. Then the aircraft cruises for 10 minutes at a power loading of 0.083 kW/kg. The aircraft then lands with a power loading of 0.25 kW/kg for 30 seconds and taxis in under a power loading of 0.0083 kW/kg for 30 seconds. Then, this mission is repeated. Finally, there is a 20-minute cruise reserve. The mission segment time durations are based on missions proposed by Patterson et al. [18], and the power loading is derived from McDonald and German [19].

Each type of aircraft has a different set of assumed power loading parameters. In Table 2, the power loading for each flight segment is listed for each type of aircraft considered: the quadrotor, tiltrotor/tiltwing, lift plus cruise, and side-by-side helicopter. These power loading numbers are derived from the takeoff and cruise power requirements presented by McDonald and German [19].

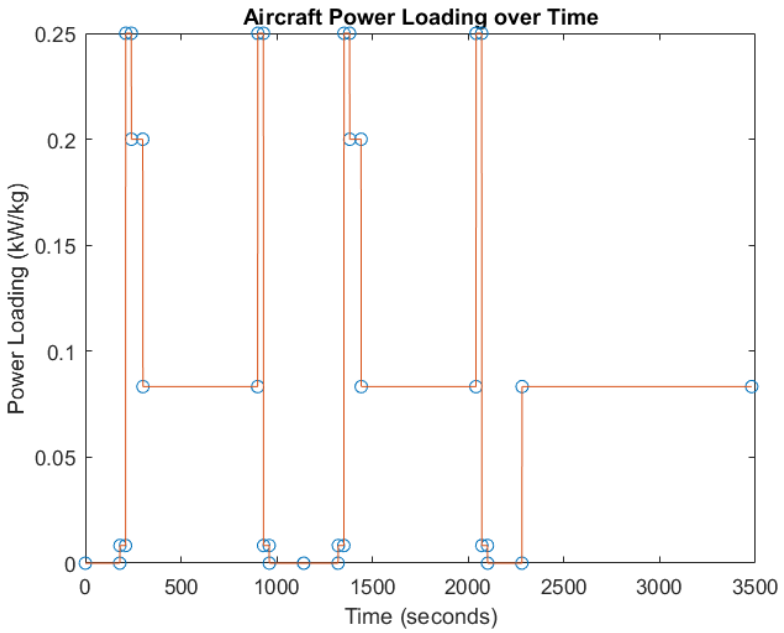

Figure 1. Example aircraft mission profile shown as power loading over time.

Table 2. Power Loading Assumptions for Each Flight Segment

Parameter/Mission Segment	**Quadrotor**	**Tiltrotor/Tiltwing**	**Lift Plus Cruise**	**Side by Side**
pVTOL (kW/kg)	0.125	0.25	0.25	0.125
pClimb (kW/kg)	pVTOL	(pVTOL/4)*1.5	(pVTOL/3)*1.5	pVTOL
pCruise (kW/kg)	pVTOL*1.5	pVTOL/4	pVTOL/3	pVTOL
pTaxi (kW/kg)	0.1*pCruise	0.1*pCruise	0.1*pCruise	0.1*pCruise
pLoad (kW/kg)	0	0	0	0
pCharge (kW/kg)	-0.2	-0.2	-0.2	-0.2

For an all-electric battery-powered vehicle, an initial guess is made for the MTOW of the vehicle (2*target payload) and the battery is first sized by power and the aircraft run through the mission. The battery capacity is updated based on the energy used, and the vehicle is run again until both power and energy requirements are satisfied. The resulting payload is determined and the MTOW guess updated based on the error in payload. The sizing is run until the error between achieved payload and target payload is less than 2 kg. The hybrid-electric vehicle sizing involves the same process; however, iteration of both the augmentation battery and the fuel tank are performed to ensure the augmentation battery meets power and energy requirements while the tank is run to empty at the conclusion of the sizing mission. An example of the sizing output for a battery-only vehicle is shown in Figure 2. The battery state of charge is shown depleting at different rates for different parts of the sizing mission in Figure 2a. The relative fraction of the "structure," which includes everything but payload and battery, is shown relative to the battery and payload fractions in Figure 2b.

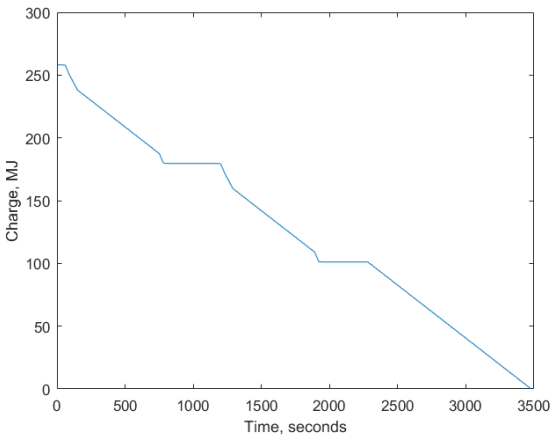

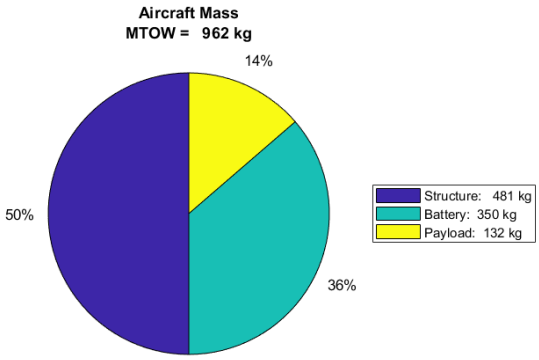

a) Battery state of charge during sizing mission. b) Battery vehicle mass fractions.

Figure 2. Example output of the sizing mission for a battery-only vehicle.

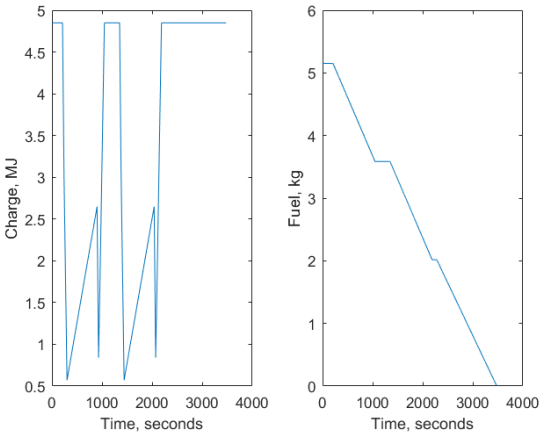

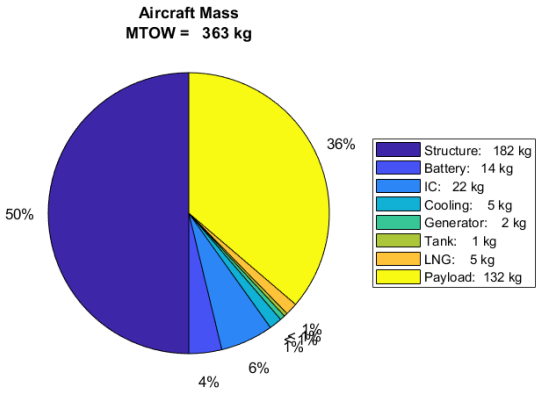

a) Battery and fuel during sizing mission. b) Fueled vehicle mass fractions.

Figure 3. Example output of the sizing mission for an LNG-IC vehicle.

Given the same sizing mission, Figure 3 is an example of the output from sizing an LNG-IC vehicle. In Figure 3a, the fuel is observed depleting to zero while the battery charge remains above zero (sizing was successful because the battery is capable of performing the mission, and the fuel tank contains just enough fuel to meet mission and reserve requirements). In Figure 3b, the mass of the vehicle, sized with the same mission, is significantly less than the all-battery option shown in Figure 2b. The structure fraction is the same (this is set to 50 percent) but the payload fraction is much higher.

3. Carbon Dioxide Emission Calculation Assumptions

Carbon dioxide (CO_2) emissions are considered in the results below. The CO_2 generation rates shown in Table 3 were used for the various fuels considered. These represent the CO_2 that will be generated by the energy loaded onto the aircraft. For comparison purposes, imagine that that electricity will be converted to useable mechanical energy at around 94 percent efficiency while

the LNG or diesel may be at around 30 percent. For electricity, the rate of CO_2 emissions was selected to represent the present California grid emissions, currently one of the cleanest of the 50 states, because the region under consideration was the San Francisco Bay Area. The CO_2 emissions for the fuels represent the CO_2 released by burning the fuel and releasing one MJ of thermal energy.

Table 3. CO_2 Emissions Rates

Energy Type	CO_2 Emissions
Electricity	78.2 g CO_2/MJ (CA grid)
LNG	53.6 g CO_2/MJ (raw)
Diesel	74.1 g CO_2/MJ (raw)

4. Model Limitations

One limitation of this analysis is the assumption that the aircraft structure, motors, and props make up a fixed percentage of the vehicle, with the remaining portion consisting of the power system, energy storage, and payload. For the results presented in this section, the structural mass fraction was assumed to be 50 percent for all configurations, for lack of better numbers at the time the model was run. Subsequent modeling of the lift plus cruise and tiltrotor/tiltwing use structure fractions of 51.2 percent and 39.3 percent, respectively. These structure fractions were selected by comparison to the weight fractions of a tiltwing vehicle and the lift-plus-cruise concept vehicle presented by Silva [20].

An additional limitation of the analysis is that the weight of the fueled aircraft does not decrease as fuel is used. Rather, the weight is constant for both fuel-based and battery-powered aircraft. This constant weight assumption leads the fueled vehicles to consume slightly more fuel than would be expected. This limitation implies that when comparing results between battery-electric and fueled vehicles, the battery-electric vehicles will appear somewhat more favorable than if the fueled vehicles decreased in weight over time. This will be corrected in future versions.

B. Propulsion System and Energy Storage Type Comparisons

Before moving into a full UAM network simulation, it is instructive to study the general tradeoffs between the various energy storage and propulsion system types. A tiltrotor vehicle was sized to a mission consisting of a single partial cycle (i.e., takeoff and cruise) for various cruise durations and three separate payloads to illustrate how the MTOW and CO_2 emissions vary. Only takeoff and cruise were used because takeoff largely determines system power requirements and cruise sets energy requirements.

The results in Figure 4 through Figure 6 compare battery-powered vehicles with LNG and diesel vehicles using IC engines, turbines, or SOFC systems at three scales: one, two, and four passengers. In each of the following three figures, MTOW is plotted against design endurance for each technology type in subfigure a), and the CO_2 generation rate in grams CO_2 per minute is plotted against design endurance for each technology type in subfigure b).

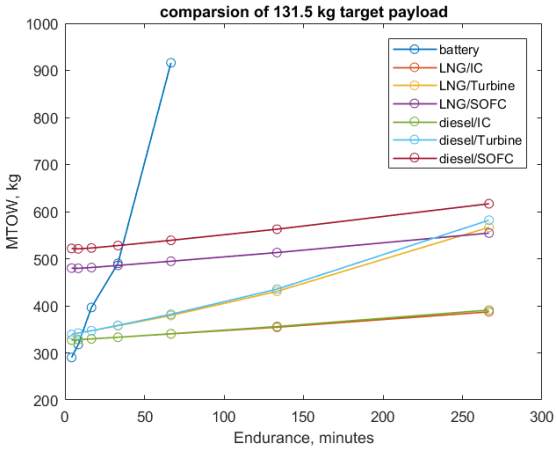

a) MTOW vs. endurance.

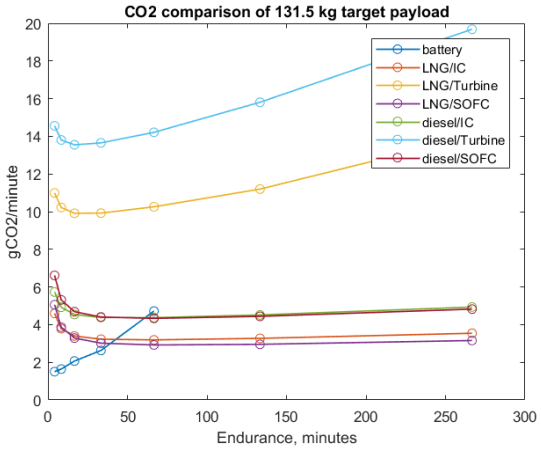

b) g CO_2/minute vs. endurance.

Figure 4. Comparison of one-passenger (i.e., 131.5-kg or 290-lb payload) vehicles.

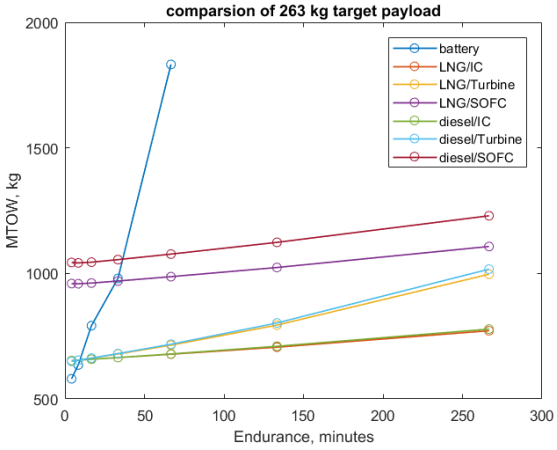

a) MTOW vs. endurance.

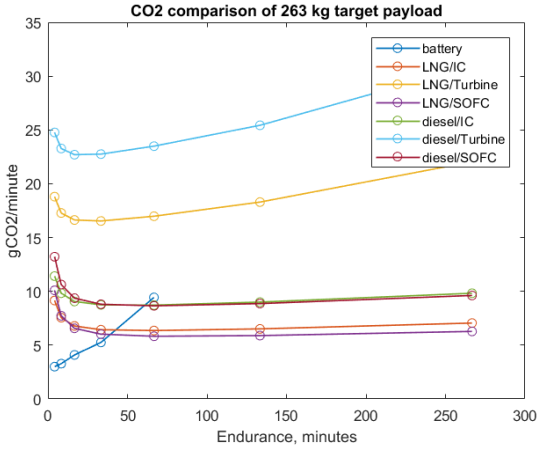

b) g CO_2/minute vs. endurance.

Figure 5. Comparison of two-passenger (i.e., 263-kg or 580-lb payload) vehicles.

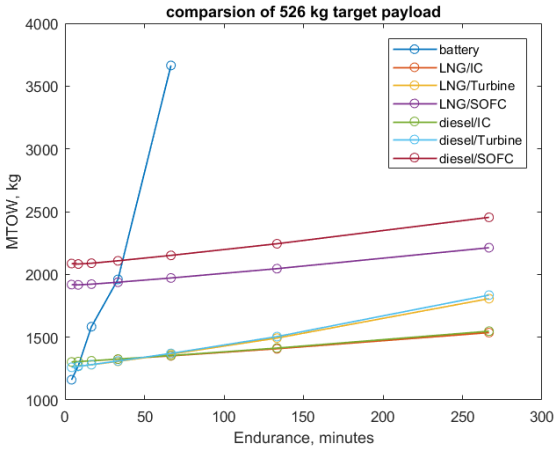

a) MTOW vs. endurance.

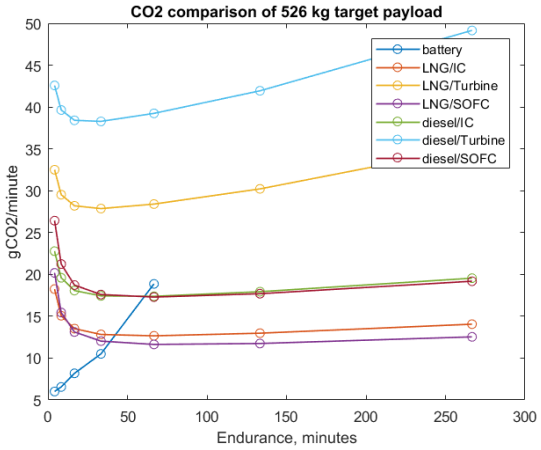

b) g CO_2/minute vs. endurance.

Figure 6. Comparison of four-passenger (i.e., 526-kg or 1160-lb payload) vehicles.

For nearly all endurances at one, two, and four passengers, the IC engine results in the lowest weight, followed by the turbine. The battery vehicle is lighter than the SOFC vehicle for endurances of up to approximately 30 minutes, but the SOFC becomes lighter than the battery vehicle for longer endurances. The battery vehicle sizing only closes (i.e., feasible, non-near-infinite weight vehicles result) at endurances of approximately 66 minutes and below. For endurances under 33 minutes, the battery vehicle exhibits the lowest CO_2 emission rate. At higher endurance, the LNG/IC and LNG/SOFC have comparable CO_2 generation rates to one another, with the SOFC resulting in slightly improved emissions. While the IC engine is significantly less efficient than the SOFC, the lighter weight of the IC aircraft reduces the required fuel burn and leads carbon emissions of the IC to be similar to the SOFC, though the SOFC still results in slightly lower emissions than the IC engine. The next highest CO_2 rates are the diesel IC and diesel SOFC. The turbines, because of the small size of the system, are very inefficient and result in the highest CO_2 production rates.

III. NETWORK MODEL

In order to assess the performance of different vehicles within a vertiport network, a full UAM network simulation was built. The UAM network is defined by the locations of vertiports, the relative demand expected at each vertiport (which is defined by "weighting" factors stating the probability of a trip originating or ending at the vertiport), and the number of pads at the vertiport that are available for takeoff/landing, parking, and replenishment.

A. Metropolitan Area Representation

A vertiport network is defined using a .kml file exported from a My Map© by Google [21]. The vertiport locations are those described by Daskilewicz et al., and more information on location selection and origin/destination weightings is available in reference [22].

1. Vertiport Site Selection

The San Francisco Bay Area was selected for study with the network model. This region is a large metropolitan area that includes several major city centers, significant surrounding urban sprawl, and is largely constrained by existing infrastructure—the San Francisco Bay and several mountain ranges. A map of vertiport sites is shown in Figure 7. Folsom is not included in the map or the simulation; the battery-powered vehicles had trouble closing because of the long distance to the Folsom vertiport.

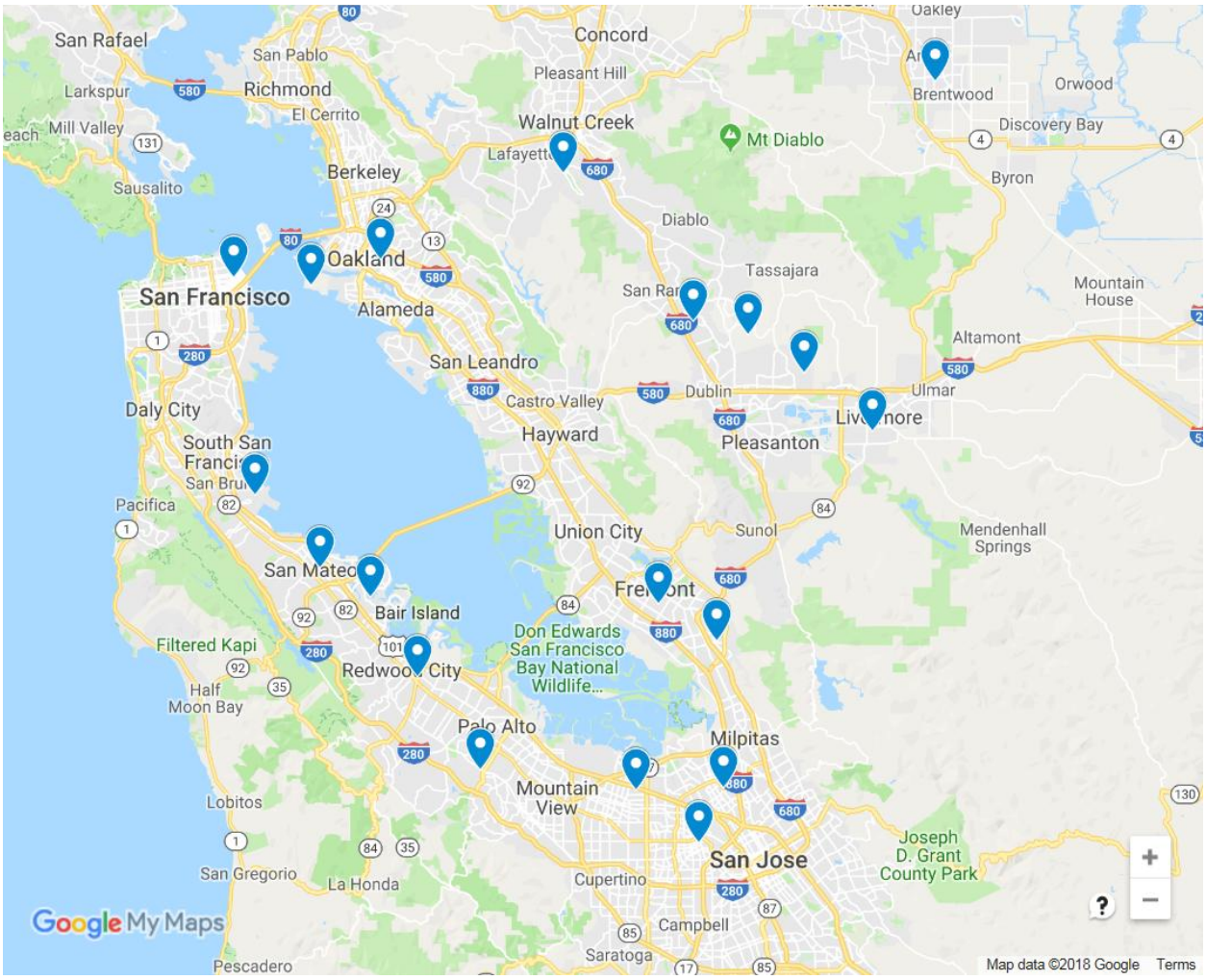

Figure 7. Map of proposed vertiport sites in the San Francisco Bay Area.

The GPS coordinates, origin and destination weighting, and number of pads for each vertiport are shown in Table 4. The GPS coordinates are used to calculate mission distance; distance along with speed and routing factor (see Table 5) are used to calculate time between each of the vertiports. Weighting is used in the demand generation algorithm, which is described in more detail below. The number of takeoff and landing (ToL) pads were selected to reduce bottlenecks at the vertiports based on experimental runs of the simulation.

2. Other Parameters

There are many other relevant parameters to the network simulation. Table 5 lists these parameters needed to run the model. Many of these parameters are discussed in later sections.

Table 4. Vertiport Parameters

	Location		**Weighting**					
Name	Latitude	Longitude	Origin	Destination	#ToL pads	#Replenish	#Parking	Special
Oakland	37.80448996	-122.2582997	15	61	8	8	16	
Fremont	37.53653094	-121.9869842	52	34	12	8	16	
Weibel	37.50875569	-121.929619	15	3	4	8	16	
Doolan Canyon	37.71648155	-121.8433985	20	20	4	8	16	
Livermore	37.67114195	-121.7760421	42	20	12	8	16	
Brentwood	37.94220798	-121.7149882	19	6	4	8	16	
San Ramon	37.75696664	-121.9527965	21	24	4	8	16	
Walnut Creek	37.8703056	-122.0794298	18	22	4	8	16	
Bollinger Canyon	37.74553802	-121.8986608	23	6	4	8	16	
Folsom	38.67095983	-121.1417955	4	5	0	0	0	Not used
San Francisco Financial District	37.79031415	-122.4024319	14	33	4	8	16	
Alameda	37.78419086	-122.327654	0	0	4/16*	8	16	*Depot
San Mateo	37.56567723	-122.3183091	25	23	12	8	16	
Foster City	37.54197722	-122.2686095	29	23	8	8	16	
Redwood City	37.48046752	-122.2225149	20	23	4	8	16	
SFO Airport	37.62146198	-122.3823131	32	26	16	8	16	Airport
North San Jose	37.3939046	-121.9218031	6	7	4/12*	8	16	*Depot
SJC Airport	37.35123421	-121.946514	16	27	12	8	16	Airport
Sunnyvale	37.3923169	-122.0086362	9	8	4	8	16	
Palo Alto	37.40819168	-122.1615997	3	12	4	8	16	

3. Distance to Flight Time

The description of each vertiport in the .kml file contains a tag that indicates several parameters for that vertiport including the number of landing pads, number of replenishing stations (if used), the number of pads for parking, the origin and destination demand weightings, and the vertiport type. The .kml file also includes the GPS locations of the vertiports and the names of the vertiports. All of this information is parsed and loaded into the city model. The Haversine distance (distance between two points on the surface of a sphere) is then calculated for each vertiport pair. That distance is then multiplied by the routing factor, a number that is a correction factor to take into account deviation from straight-line flight paths to route around obstacles. The routing factor that was used corresponds to the value presented by Moore [3]. Finally, the specified vehicle cruise speed is used to convert from distance to flight time. Real flight time along with all other times, such as mission segment times including loading, takeoff, climb, landing, and taxi, are converted to integer time steps.

Table 5. Other Relevant Network Model Parameters

All	Name	Value	Description
	num_people	10000	number of people in the system
	ratios	[.4,.1,.5]	commuter, churn, airport transfer
	parking_fraction	0.25	fraction of filled parking spaces below which rebalance is triggered
	max_wait_time_dispatch	300	time a person will wait before a vehicle is dispatched
	max_wait_time	300	time a vehicle will wait to be filled
	speed	208.35	km/hr
	people_per_vehicle	7	nominal people-flights per aircraft
	new_time_step	30	time step
	routing_factor	1.42	additional distance multiplier for each route [3]
	prediction_correction	1.6	adjustment for fuel use prediction
	rebalance	1	rebalance, yes or no
	new_demand	1	generate new demand, yes or no
	timers	[180,30,30,60,30,30,180]	load, taxi out, takeoff, climb, land, taxi in, unload
	max_iterations	100	
	tVTOL	30	seconds in VTOL mode (sizing only)
	tCruiseReserve	1200	seconds cruise reserve (sizing only)
	tClimb	60	seconds in climb mode (sizing only)
	tCruise	1200	seconds in cruise (sizing only)
	tTaxi	30	seconds in taxi in or out (sizing only)
Battery	reserve_limit_bat	0.99	limit below which recharge occurs
	recharge_rate	200	kW, rate for battery recharge
	nCycles	1	number of flights to run for sizing mission
Fuel	replenish_at_depot	16	override number of refuel stations at depots
	reserve_limit_fuel	0.25	limit below which refuel occurs
	refuel_rate	1	kg/sec, rate of refueling
	recharge_in_flight	1	Boolean, allows battery recharge in flight
	nCycles	8	number of flights to run for sizing mission

4. Model Limitations

The city model contains a number of assumptions that introduce inherent limitations of its ability to model all the intricacies of realistic UAM operations. The model could be used to provide insights into the impacts of preliminary selections on vehicle and network performance, and over time many of these limitations will be addressed with additional modeling fidelity. A few of the more important limitations of the model, and how results could deviate from real-world operations, are discussed.

First, the model vastly oversimplifies the complex airspace integration issues that must be solved prior to realizing UAM. Specifically, the model assumes that UAM air traffic can be deconflicted and safely separated from all forms of air traffic (including aircraft outside of the UAM

network). The model assumes that aircraft will fly some distance farther on average than the direct distance between vertiports to allow for safe airspace integration. This increased flight distance is accounted for via a "routing factor," which was set to 1.42 for the work presented in this paper, that multiplies the direct distance between origin and destination. The model does, however, handle interactions of vehicles at the vertiports, i.e., no two aircraft can occupy the same ToL pad, replenishing, or parking pad at the same time. If an aircraft arrives at its destination while other aircraft are occupying the ToL pads, the aircraft loiters (at a power setting equivalent to cruise) until a pad is free and a landing can ensue.

All vehicles in the network are the same. The capacity to model multiple vehicle types does not currently exist; for example, simultaneously modeling vehicles with different numbers of seats in the same model or using a mix of battery and fueled vehicles.

There is no stochastic nature to the mission segment times modeled. Mission durations are directly calculated from distance, speed, and routing factor. Variations in speed or routing are not taken into account. Also, variations in other flight segments are not captured.

B. Aircraft Sizing Method for Network Simulation

Although aircraft were originally sized to the same mission as described previously in Section II.A.2, early exploration of the network performance with aircraft sized to these missions and practical operational considerations led to modification of the sizing missions for both battery-electric and hybrid-electric vehicles.

Early simulations with battery-electric vehicles sized to cruise lengths of 10 minutes, as discussed previously, indicated that these vehicles could not fly the longer routes within the San Francisco Bay Area network described in Section III.A.1. Additionally, to keep the mass of the battery-electric vehicles from growing too significantly, it was assumed that every vertiport would have charging infrastructure so that the aircraft could be sized to only a single flight cycle with a 20-minute reserve, which corresponds to existing Federal Aviation Regulation requirements for rotorcraft under visual flight rules (14 CFR § 91.151). With these assumptions, the sizing mission for the battery-powered aircraft is shown in Figure 8, which represents a single 20-minute mission with a 20-minute-cruise reserve.

Because the size of a hybrid-electric vehicle does not increase very significantly as the endurance of the vehicle is increased (as shown in Section II.B), it seems logical to size hybrid-electric UAM vehicles to perform multiple missions prior to needing to refuel. Additionally, storing fuel at every vertiport may be impractical from a fuel distribution logistics standpoint, and it is a potential safety hazard to have fuel stored at every vertiport. Consequently, there is the ability to allow hybrid-electric vehicles to refuel at a (or one of multiple) centralized refueling depot(s) in a metropolitan area or at only specific vertiports where fuel storage may not be problematic (e.g., one co-located at an existing airport). With these considerations, and after early initial simulations of the San Francisco Bay Area UAM network, the nominal number of 20-minute cycles for the fueled vehicles was selected to be eight, which is one more than the average number of missions that a one-seat aircraft would fly in a day. An example of the eight-cycle mission is shown in Figure 9. This sizing mission minimizes the number of times a vehicle needs to refuel during the day, without sizing the vehicle with an excessive fuel capacity.

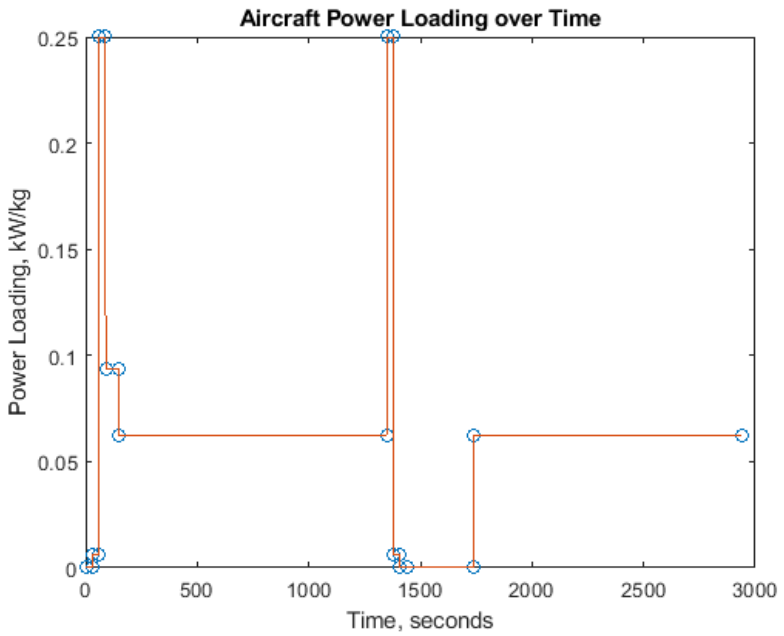

Figure 8. Single-cycle sizing mission for battery-powered vehicles.

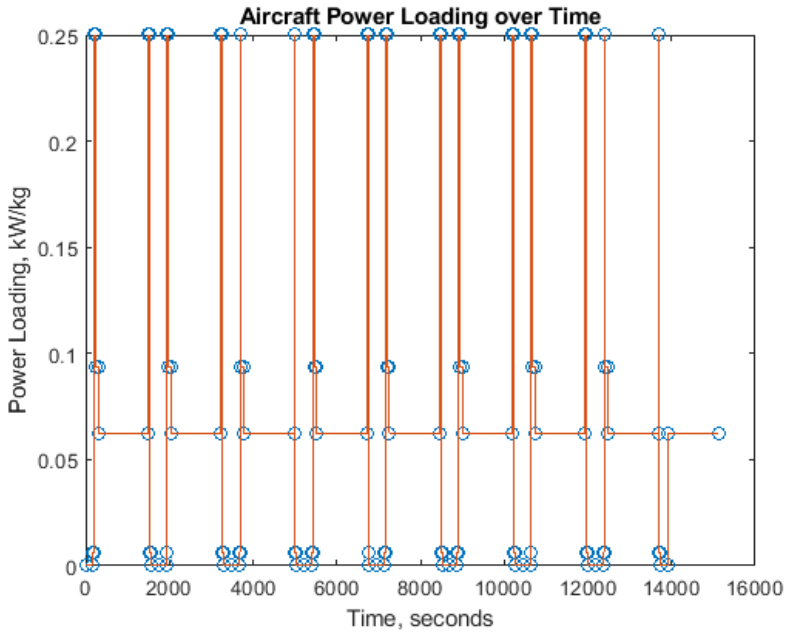

Figure 9. Example eight-cycle sizing mission for fueled vehicles.

C. Demand Model

The demand model is based on the creation of individual people with different demand types. Three types of demand—commuter, churn, and airport transfer—are modeled. A commuter takes two trips: one in the morning, likely from home to his/her place of work, and one in the evening, returning to his/her origin. Churn demand models a person who takes a single trip from one point to another and represents trips such as an urgent business meeting across town. An airport transfer either takes a trip to an airport or from an airport.

1. Request Timing Generation

Trip requests are generated in one of three ways, depending on the type of demand.

The first type of demand, commuter, creates two trips. The first occurs sometime in the morning, defined by a normal probability distribution centered at 8:00 AM with a standard deviation of 2 hours. The second commuter trip occurs in the evening, defined by a normal probability distribution centered at 5:00 PM, with a standard deviation of 2 hours.

A churn trip is generated on a time distribution that is at a constant probability between 5:00 AM and 9:00 PM. Prior to 5:00 AM, the probability distribution is defined by half of a normal distribution with a peak at 5:00 AM and a standard deviation of 1 hour. Similarly, after 9:00 PM, the demand is modeled as half of a normal probability distribution with a mean of 9:00 PM and a standard deviation of 1 hour. This is called a "flat normal distribution" since it is a uniform distribution terminated with normal distributions. This distribution was chosen to provide a base level of activity in the network that was tied only to people being awake for the day and having a desire to take a trip to some location.

For the purposes of this modeling, the airport transfers were generated with a distribution of normal probability distributions, on a normal probability distribution centered at 12 PM with a standard deviation of 6 hours. The smaller normal distributions had a magnitude between 90 and 270 and a standard deviation between 0.2 and 1.0 hours. This distribution of distributions was used to generate the time requests in such a way that the "peakyness" of airport transfer demand could be captured. An example of the normal distribution of normal distributions is shown in Figure 10.

2. Origin and Destination Selection

The selection of origin and destination also depends on the type of demand: commuter, churn, or airport transfer.

There are two trips associated with a commuter—the morning commute and the evening commute. Each commuter's morning origin and evening destination are the same vertiport, and this vertiport is randomly determined by the port origin weighting during the morning. The destination for the morning trip, and therefore the origin for the evening trip, is determined randomly by the port destination weighting during the morning commute multiplied by a distance weighting function. Vertiports with a high origin weighting tend to be residential areas, and vertiports with a high destination weighting tend to be areas with many places of work. The distance weighting function takes the form of Equation 1, consisting of four fit parameters, a, b, c, and d, and the $distance$. This has the effect of de-emphasizing very short commute trips and

very long commute trips. The effect of the distance weighting function is demonstrated by the trip demand distance histogram shown in Figure 11. Because of the stochastic nature of the demand generation and the influence of origin/destination weighting, the distribution only roughly fits the weighting function, w_d, where a is 1/367.8791, b is 0.001, c is 2, and d is 2.

$$w_d = a * (distance^c) * \exp(-b * distance^d) \quad \text{(Eq. 1)}$$

A churn trip origin is generated randomly from all existing vertiports regardless of origin weighting. Similarly, the churn trip destination is generated randomly from all existing vertiports regardless of destination weighting.

An airport transfer trip will have either an origin or destination at a vertiport collocated with an airport. The determination of whether the airport is the trip origin or destination is randomly determined, and the probability of the origin or destination being the airport is equal. When there is more than one airport, the airport used as the origin or destination is randomly selected from all vertiports located at airports. The corresponding origin or destination is then randomly selected from all vertiports. For the purposes of the modeling in this paper, the relative ratios of these types of trips were assumed as 40 percent commuter, 10 percent churn, and 50 percent airport transfer.

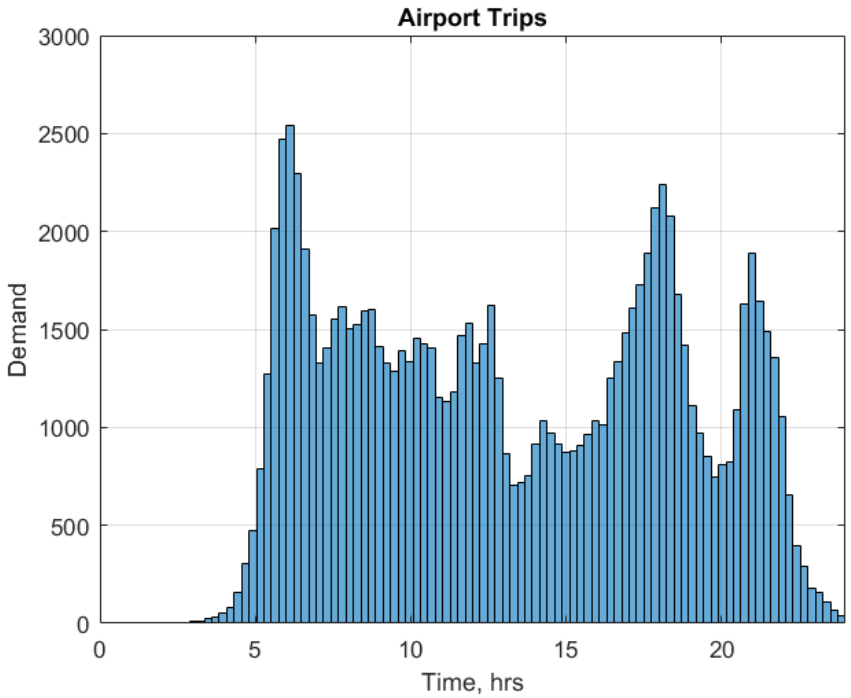

Figure 10. Example normal distribution of normal distributions; each small distribution represents the demand for a UAM flight generated by an aircraft arrival or departure from an airport.

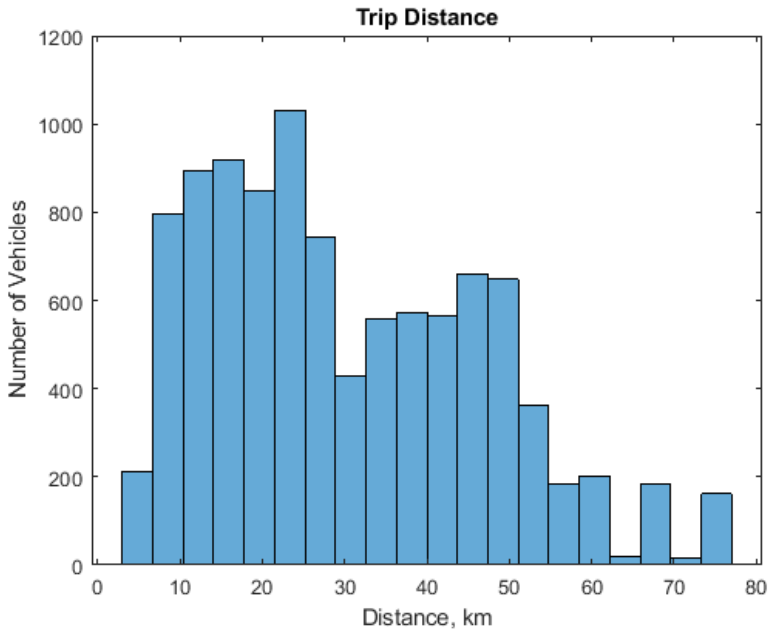

Figure 11. Trip distances as a result of the demand generation algorithms including the distance weighting function.

3. Model Limitations

The demand model depends on the origin and destination weighting to create commuter-based morning influx and evening outflow of people to and from city centers. Churn creates random trips throughout the day. Airport transfers create airport-focused movement of people in the system. The relative number of each type of trip and the specific probability distributions for each demand type were selected fairly arbitrarily to demonstrate how the model can be used. As this work is refined, hopefully more detailed information will be obtained that can better inform the timing probability distributions for each trip type, the origin/destination selection, and the relative ratios of the number of each person type. These characteristics will vary for each metropolitan area studied.

D. Dispatch Model

One of the most important aspects of an on-demand UAM network model is the dispatch model, i.e., the model that dictates when an aircraft departs from a vertiport and the destination of the trip. This model will ultimately determine two major characteristics of the system: average wait time and average load factor (ALF). The average wait time refers to the average amount of time a passenger must wait from demand request until the flight departs, considering all flights in the network over the course of a day. The ALF is the number of seats filled with paying passengers divided by the total number of available seats on all flights throughout the entire network in the day.

In general, the ALF and average wait time can be traded. For example, for a multi-passenger vehicle, the departure of the vehicle could be delayed until a specified number of people are on board, which would have the effect of improving ALF at the cost of average wait time. However, in this simplistic scenario, it is possible that an insufficient number of passengers may arrive during the operating day for the aircraft to depart with the specified number of passengers, which could leave certain passengers stranded. Clearly, such a result would be unacceptable. To alleviate the issue of stranded passengers and provide a more acceptable means of operation, multi-passenger vehicles could delay departure until a specified number of people are on board or until the first passenger has been waiting a predefined amount of time. In this second scenario, the tradeoff between filling the aircraft with more paying passengers and reducing the first passenger's wait time is clear. Ultimately, if the wait time becomes too large, passengers would no longer benefit from a speed advantage by taking the aerial transportation mode, and the UAM service would fail. Furthermore, since the DOC per passenger-kilometer is related to ALF, the dispatch model can have a major impact on the price the operator would need to charge passengers to cover the DOC. The remainder of this section discusses the dispatch model employed in the simulations.

1. Dispatch Model Implementation

The dispatch model is based on heuristics that seek to balance the ALF and average wait time across the entire UAM network. The primary assumption of the dispatch model is that trips are purely on demand, i.e., there is no prior knowledge of when a trip will be requested, and the request is logged when a person arrives at the vertiport. When a trip is logged, a vehicle will be immediately dispatched if available and if the vehicle is full.[**] If the vehicle is not full, then the vehicle will wait a maximum of 300 seconds (5 minutes) before being dispatched with a load factor of less than 1.0.

In addition, there is a "rebalancing" process that can be initiated to help ensure that aircraft are moved between vertiports to best satisfy demand across the entire UAM network. If the demand at a particular vertiport exceeds the ability of all "available" aircraft at that vertiport to meet the demand, then a rebalancing is initiated. The number of available aircraft is the number of aircraft ready at the vertiport plus the number of aircraft in route to that vertiport. Additionally, if the number of available aircraft at a vertiport is less than 25 percent of the number of parking spaces at the vertiport, then a rebalancing is initiated.

When a rebalancing is initiated, there is an attempt to dispatch a vehicle from the "targeted vertiport" to the vertiport initiating the request. A rebalance request will only be successful if the number of available aircraft at the targeted vertiport is less than demand at that vertiport. The targeted vertiport, which will dispatch a vehicle to the vertiport with the deficit, is selected based on its proximity to the vertiport initiating the rebalance request and its type, i.e., if it is a depot or not.

For simulations with only battery vehicles, it is assumed that every vertiport has charging infrastructure so that there are no depots. In this scenario, the targeted vertiport is initially selected as the one closest to the vertiport that initiated the rebalance request. If that vertiport cannot provide a vehicle because of high demand, the next closest vertiport then becomes the

[**] One-passenger vehicles dispatch immediately upon the trip being logged.

targeted vertiport. If that target vertiport cannot provide a vehicle, the process continues targeting vertiports farther and farther from the vertiport with the deficit until the rebalance request is satisfied or all possible targeted vertiports have failed to dispatch a vehicle.

For simulations with depot-based replenishing, which in these simulations is the case with all fueled vehicles, the first targeted vertiport is selected as the closest depot to the vertiport initiating the demand request. If this depot does not have any aircraft it can supply, the next targeted vertiport would be the next closest depot. If demand cannot be met by any of the depots, then the closest non-depot vertiport is targeted, and the process then continues as in the case described previously with no depots.

Finally, in any network with depot-based refueling, consideration of when the vehicles are dispatched to the refueling depot is required. Vehicles with fuel below a predefined reserve level, which is set at 25 percent for these simulations, are automatically sent to a depot to refuel. Additionally, before each potential flight, the estimated fuel usage of completing the proposed mission plus then proceeding to the refueling depot nearest to the destination vertiport is considered. If this fuel usage would result in the fuel dropping below the reserve level, the vehicle is routed directly to the depot closest to the aircraft's current location instead of performing the mission.

2. Model Results

To study how vehicle design choices impact the ALF and average wait times, UAM network simulations were performed with tiltwing/tiltrotor vehicles with different propulsion systems and fuel types. Additionally, comparisons of the ALF and average wait times in cases with both autonomous and piloted aircraft were performed, and results from all of these simulations are described in this section.

The average wait time and ALF results were nearly identical when comparing piloted and autonomous tiltwing/tiltrotor vehicles using different power systems. This result is as expected since the presence of the pilot only increases the payload of the vehicle, which is then sized using the same target mission profile. Therefore, in the remainder of this section, only the results from simulations with autonomous vehicles are provided.

Differences are observed, however, between fueled vehicles and battery vehicles as illustrated in Figure 12 and Figure 13. Fueled vehicles experience a reduction in ALF and a slight increase in the average wait time because of depot-based refueling for fueled vehicles and distributed charging for battery vehicles. This is expected because fueled vehicles will occasionally make trips with no passengers on board, i.e., "deadhead flights" to a refueling depot. ALF is plotted for the autonomous tiltwing/tiltrotor, for each technology and one, two, and four passengers, in Figure 12. ALF is observed to decrease with increasing vehicle size because the dispatch model attempts to keep the average wait time reasonably low (300-second wait limit). Average wait time is plotted for the autonomous tiltwing/tiltrotor, for each technology and one, two, and four passengers, in Figure 13. Average wait time increases with increasing vehicle size because the vehicle is held until full or until the 300-second wait limit is reached.

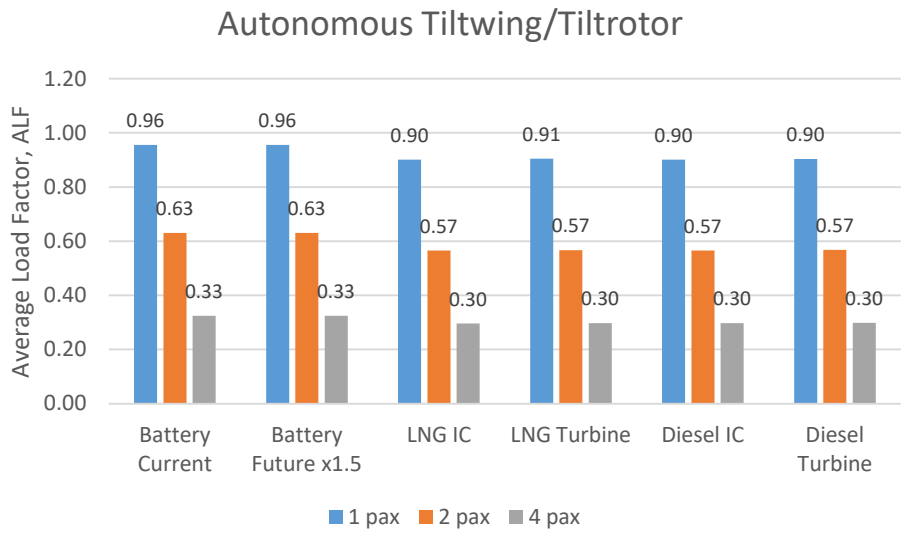

Figure 12. ALF for autonomous tiltwing/tiltrotor vehicles; variation of power technology.

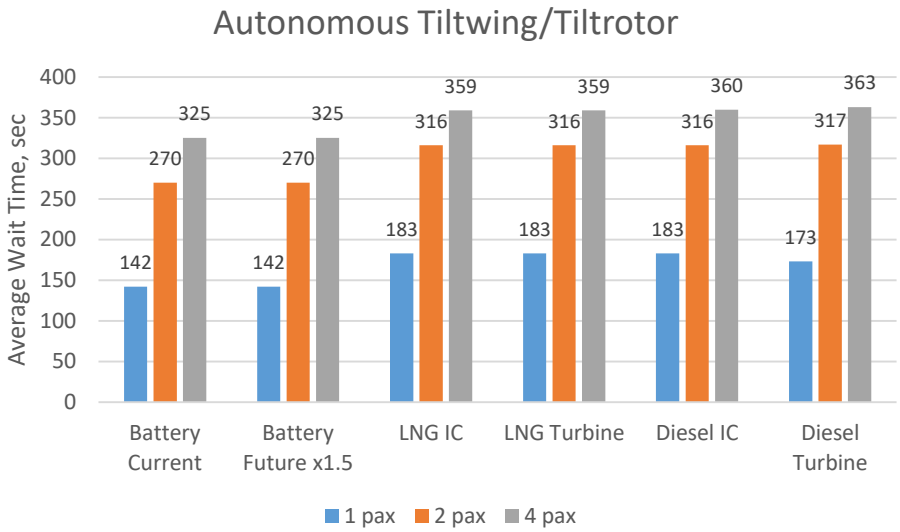

Figure 13. Average wait time (sec) for autonomous tiltwing/tiltrotor vehicles; variation of power technology.

The number of cycles for which the fueled vehicles are sized has an impact on both ALF and the average wait time. This is because, generally speaking, sizing an aircraft to fly more missions results in fewer deadhead refueling flights during operation. To explore these impacts, simulations were performed with one-, two-, and four-passenger autonomous tiltwing/tiltrotor aircraft with an internal combustion engine fueled with LNG where the number of cycles in the sizing mission was varied. Results of these simulations are provided in Figure 14 for the ALF and in Figure 15 for the average wait time. In Figure 14, the ALF is observed to increase with increasing number of sizing mission cycles because fewer refueling trips are needed. In Figure 15, the average wait time is observed to decrease with an increasing number of sizing mission cycles. Because of the reduced number of required fueling flights with increased sizing mission cycles, less time is spent waiting for a dispatched rebalancing vehicle to arrive from a depot. Beyond 12 cycles there is little change in ALF.

3. Model Limitations

The current model assumes purely on-demand operations, which would almost certainly not be the case in reality. Because trips could be reserved days, hours, minutes, or even just seconds in advance, this information could be used by the dispatch model to more strategically position aircraft around the UAM network and better satisfy demand. However, a dispatch model that considers pre-planned trips is more complex to implement. In practice, a good dispatch model would likely represent a competitive economic advantage for potential operators and, therefore, the dispatch model would be the subject of extensive development. Ultimately, the results presented above from the purely on-demand model likely represent a reasonable lower bound of the network performance that could be expected with more intelligent and complex dispatch models that may have access to pre-planned trip information.

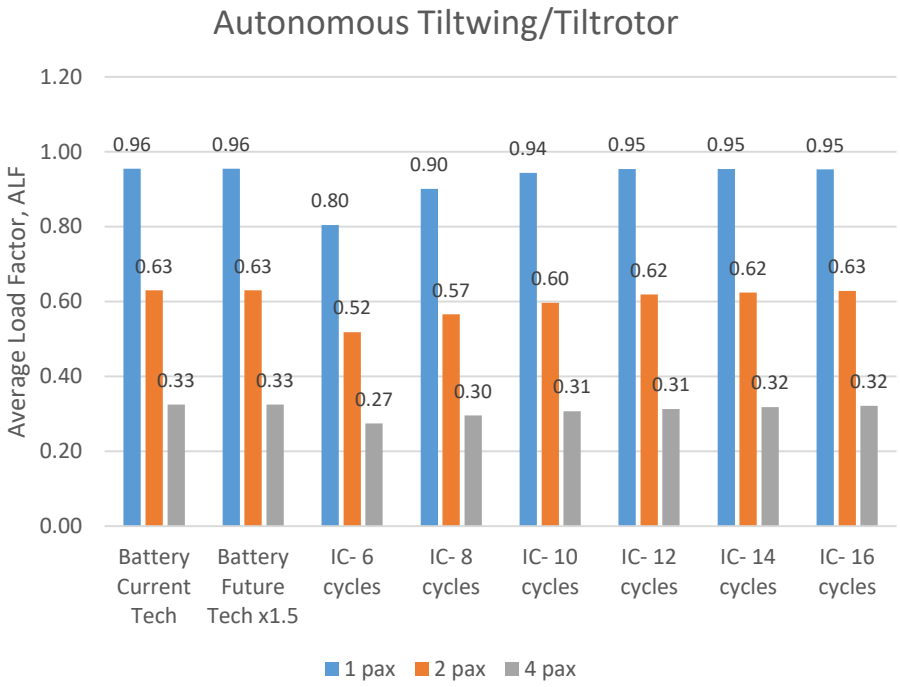

Figure 14. ALF for autonomous tiltwing/tiltrotor vehicles; variation of sizing cycle count.

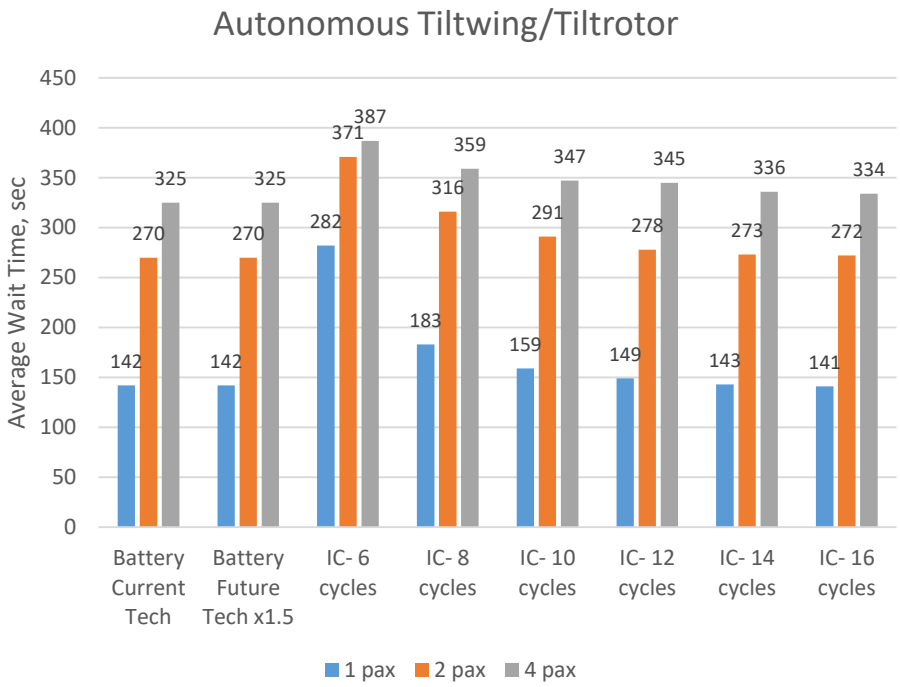

Figure 15. Average wait time (sec) for autonomous tiltwing/tiltrotor vehicles; variation of sizing cycle count.

IV. COST AND CARBON EMISSIONS STUDY

This section describes cost models and estimates the average per-passenger-kilometer costs of the various vehicles described in Section II, operating on the UAM network described in Section III. These costs are based on an acquisition cost model, an energy cost model, a maintenance cost model, and an insurance cost model, all of which are described below.

A. Cost Model Assumptions

This section describes the cost models used to estimate the ultimate per-passenger-kilometer costs of different notional vehicles operating in the network described above. An acquisition cost model by Booz Allen Hamilton [23], an energy cost model based on prices of electricity and other fuels [16], a maintenance cost model derived from reference [23], an insurance cost model, and a pilot salary model (where applicable), are employed.

1. Acquisition Cost

Total acquisition cost is modeled as the sum of the cost of the aircraft and the cost of the battery sized to that aircraft, whether it is a fully electric aircraft or a hybrid-electric aircraft. Airframe acquisition cost is based on a linear fit of aggregated cost estimates of UAM vehicle concepts presented in reference [23]. The acquisition cost (excluding battery cost) is related to MTOW as shown in Equation 2.

$$Aircraft\ Acquisition\ Cost = \frac{250000}{750} \times MTOW \quad \text{(Eq. 2)}$$

Battery cost is dependent on the design capacity that is output in the vehicle sizing process. Vehicle batteries are assumed to be priced at $400/kWh as suggested by Holden and Goel [24]. Acquisition price is not explicitly broken out for IC, turbine, or SOFC but is instead assumed to be rolled up in Equation 2. Further work is needed on the model to break out these component costs.

2. Operating Costs

The major components of the aircraft operating cost model include vehicle acquisition cost amortization, energy cost, maintenance, insurance, battery replacement, and pilot salary (assuming piloted vehicles). The vehicle acquisition cost is assumed to be distributed over a 40-percent initial down payment, followed by yearly payments with an annual interest rate of 6 percent over a 10-year vehicle lifespan [23]. Energy costs depend on usage as well as the type of energy. Energy usage is determined not only by vehicle configuration but also by network dynamics: the more efficiently a network operates (i.e., the higher the ALF), the less energy it requires. Table 6 contains energy sources employed in the model and their respective costs. In this model, it is assumed that only fully battery-powered vehicles require charging; all other vehicles are hybrid electric but do not require charging from the electric grid. Batteries are assumed to have a 2000-cycle lifetime and an acquisition cost of $400/kWh [3].

UAM vehicles are assumed to require 1 hour of maintenance per flight hour [26], with a maintenance wrap rate (labor plus overhead) of $60 per hour [23]. Based on insurance rates of conventional civil helicopters, insurance is estimated to be approximately 3 percent of the vehicle acquisition cost per year [23]. To determine pilot costs, it is assumed that pilots receive a salary of $50,000 per year, which is comparable to salaries for regional airline pilots; additionally, it is stipulated that there be 50 percent more pilots than network vehicles to account for shift changes [24].

Finally, DOC is derived from the aforementioned operating cost factors, as well as average network load factor, number of seats per vehicle, average trip length, and an assumed 250 days of operation per calendar year for each vehicle.[††] DOC is an excellent indicator of the overall feasibility of UAM vehicles and operations since it will partially drive ticket price.

Table 6. Energy Costs Rates

Energy Type	Cost
Electricity	$0.036/MJ [16]
LNG	$0.019/MJ [16]
Diesel	$0.025/MJ [16]
CNG	$0.018/MJ [25]
Jet-A	$0.031/MJ [16]

[††] 250 days per year is 4.8 days per week on average. If a vehicle is operated for 8 hours a day, 250 days a year, the yearly utilization is 2,000 hours.

B. Cost and Carbon Emissions Results

1. Direct Operating Cost (DOC)

Using the previously described cost model and network operations model, the DOC was estimated for tiltrotor/tiltwing vehicles. Recall that the network operations were modeled with electric aircraft that were sized to a single mission with 20 minutes of cruise and can recharge at every vertiport, while the fueled vehicles refuel at a centralized refueling depot and were sized to perform eight flight cycles each with a 20-minute cruise segment. Additionally, the ALFs presented in Section III.D.2 are used in the DOC calculations, which is an important point to aid in understanding some of the more counterintuitive results shown below. The tiltrotor/tiltwing configuration was selected based on comparisons of acquisition cost, which indicated that this configuration could result in the lowest acquisition cost vehicles. Similarly, only variants of the tiltrotor/tiltwing aircraft with battery, LNG, and diesel fuel were evaluated as the studies above indicate that these energy storage types have the lowest cost and/or the lowest CO_2 emissions.

Figure 16 shows the DOC in $/(pax*km) and $/(pax*mi) for one-, two-, and four-passenger vehicles with a pilot, for current battery technology, future battery technology (which is 1.5 times the current specific energy), LNG w/IC, LNG w/turbine, diesel IC, and diesel turbine. Diesel/IC and LNG/IC are relatively close in cost. All of the hybrid configurations have lower DOC than current batteries (when compared at the same passenger size) even though they have more deadhead flights to refuel at the central depot (i.e., they have a lower ALF). Additionally, most hybrid configurations also have a lower DOC than the 1.5x battery case. The lowest DOC is an IC engine with LNG across all passenger sizes.

The estimated DOC for autonomous vehicles is shown in Figure 17. Estimated DOC is significantly less for the autonomous system than for the piloted vehicles, as can be observed by comparing Figure 16 and Figure 17, for several reasons. First, the pilot salary is zero in the autonomous case. Second, the vehicle has one less seat and is, therefore, smaller, which results in lower acquisition, insurance, and energy costs. Note that the cost of the autonomous system itself is *not* included in the difference in vehicle acquisition cost, so the numbers presented in Figure 17 may be lower than would be expected in practice. Also, the insurance rate will likely be different for the autonomous aircraft, assuming lower accident rates, but this is also not included.

The number of flight cycles used to size the hybrid system was also considered, and the DOC estimates when varying the number of cycles is shown in Figure 18. Since the LNG/IC system showed the lowest DOC for all systems and the lowest CO_2 emissions among hybrid systems, the impact of the number of sizing cycles was evaluated using the LNG/IC option only. Approximately 8 to 10 flight cycles appear to be optimal from a DOC standpoint, which is due to two competing effects. First, the ALF tends to increase as the number of cycles increases, which reduces the DOC. However, the weight of the vehicle increases as the number of cycles used to size the vehicle increases, which causes more fuel to be used and thus an increase in DOC. The precise number of cycles that minimizes the DOC will likely vary for each particular network and dispatch model.

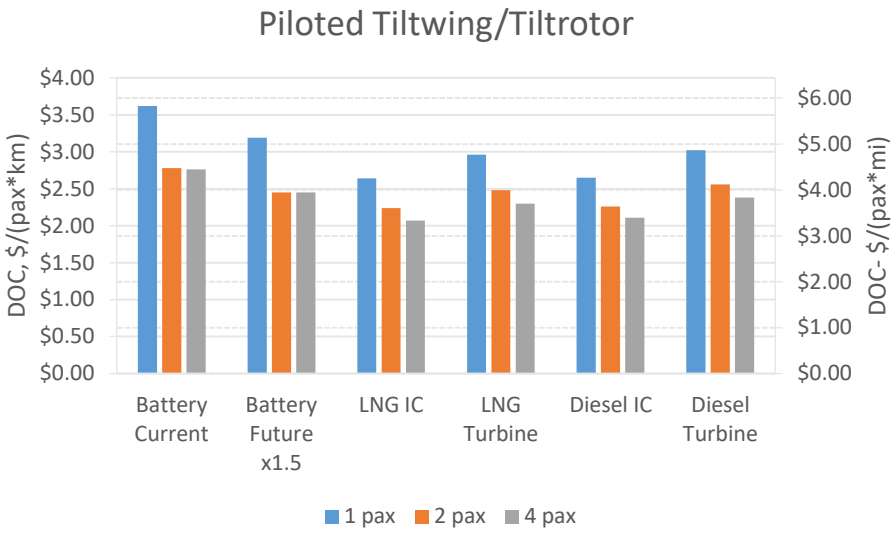

Figure 16. Piloted tiltwing/tiltrotor UAM vehicle DOC for one, two, and four passengers with different technologies.

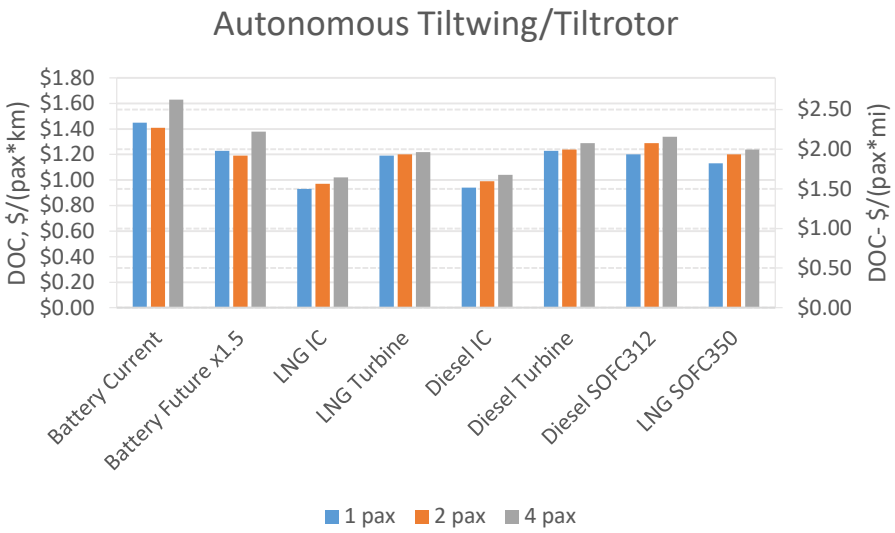

Figure 17. Autonomous tiltwing/tiltrotor UAM vehicle DOC for one, two, and four passengers with different technologies.

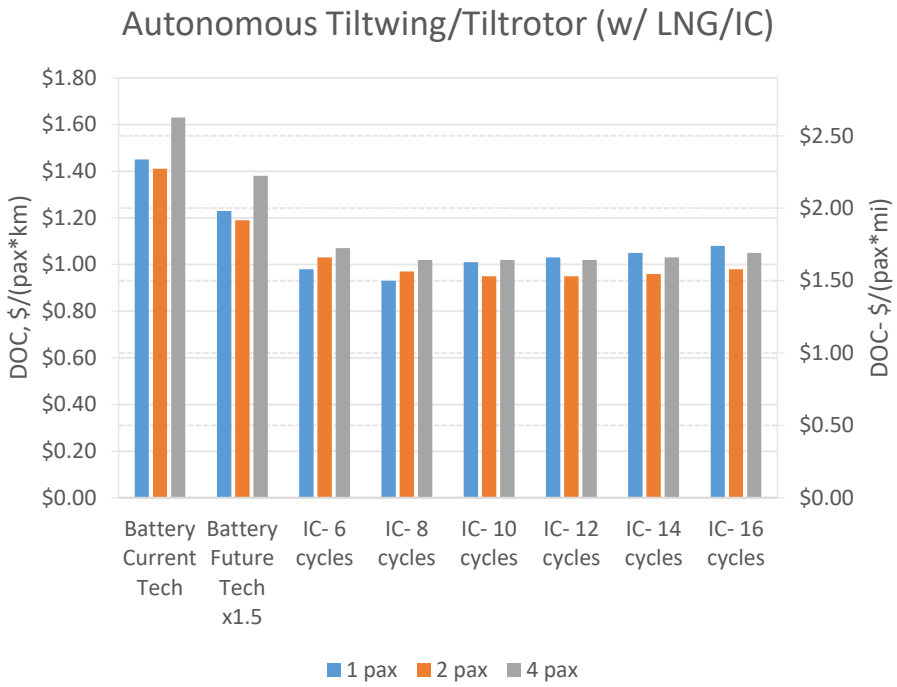

Figure 18. Autonomous tiltwing/tiltrotor vehicle DOC for one, two, and four passengers with LNG/IC for different number of sizing flight cycles; batteries are both 1 cycle.

Variations of the technology level, i.e., the specific power, of the SOFC were also explored to determine the technology level at which the SOFC might become comparable to batteries and IC engines. A near-term, diesel-fueled SOFC was considered at 312 W/kg and a near-term, LNG-fueled SOFC at 350 W/kg. Additional comparisons of LNG-fueled SOFC systems were evaluated for the midterm at 525 W/kg and for longer term at 700 W/kg. The resulting DOC estimates for autonomous tiltrotor/tiltwing aircraft are shown in Figure 19. It should be noted that the SOFC options are immediately competitive with batteries in both the near and long terms. The 700 W/kg LNG SOFC would be competitive in DOC with the LNG/IC option.

2. Carbon Emissions Results

Carbon emissions are also considered for each of the comparisons shown in Figure 16 to Figure 19. CO_2 is reported in grams/(pax*km) in Figure 20 to Figure 23. CO_2 tends to increase with the number of passengers because the ALF drops. The turbine options are the highest CO_2-emitting options because of low efficiency at these small sizes. The LNG/IC option is only slightly higher in CO_2 emissions than the battery option, calculated assuming the current California grid. Like batteries, it is possible to reduce the lifecycle emissions of the LNG/IC option through improvement of the IC engine (using turbo compounding, for example) and through the renewable production of LNG from landfill gas and other bio methanogenic sources.

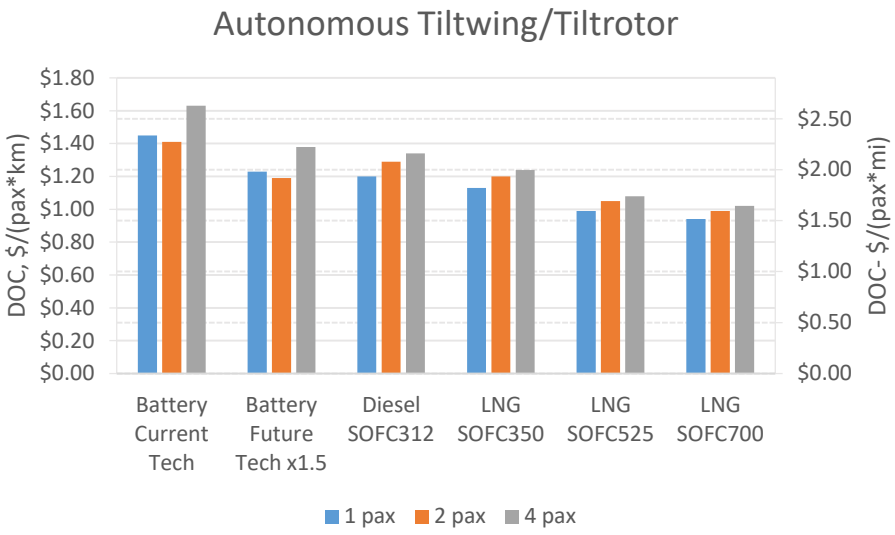

Figure 19. Autonomous tiltwing/tiltrotor vehicle DOC for one, two, and four passengers for different SOFC technology levels.

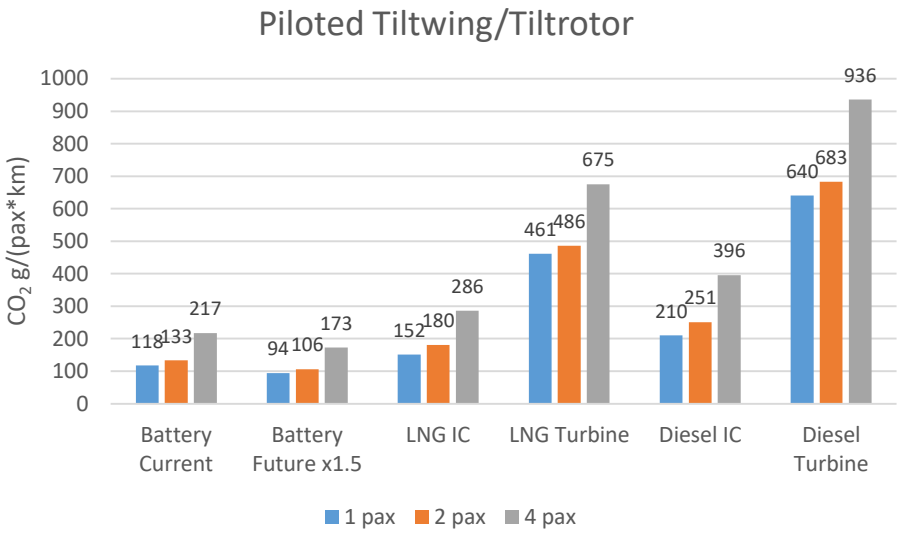

Figure 20. Piloted tiltwing/tiltrotor UAM vehicle CO_2 for one, two, and four passengers with different technologies.

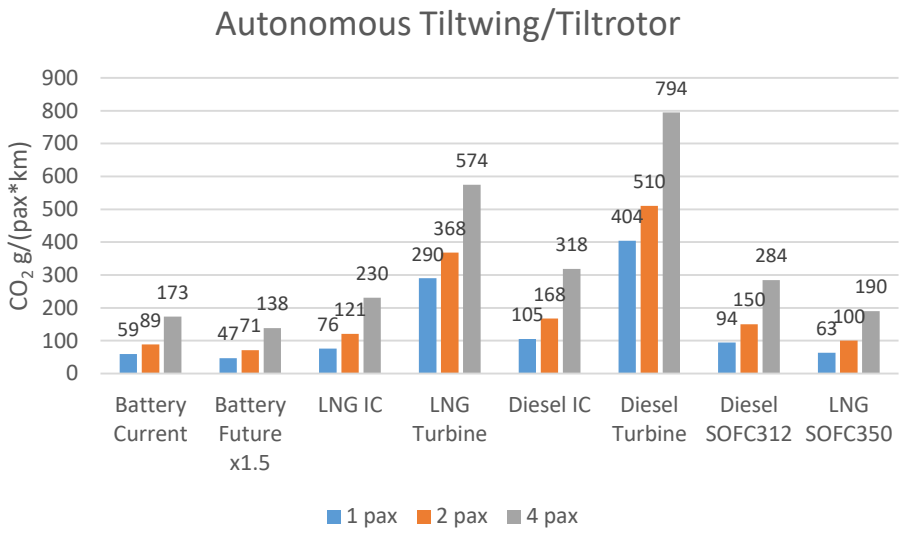

Figure 21. Autonomous tiltwing/tiltrotor UAM vehicle CO_2 for one, two, and four passengers with different technologies.

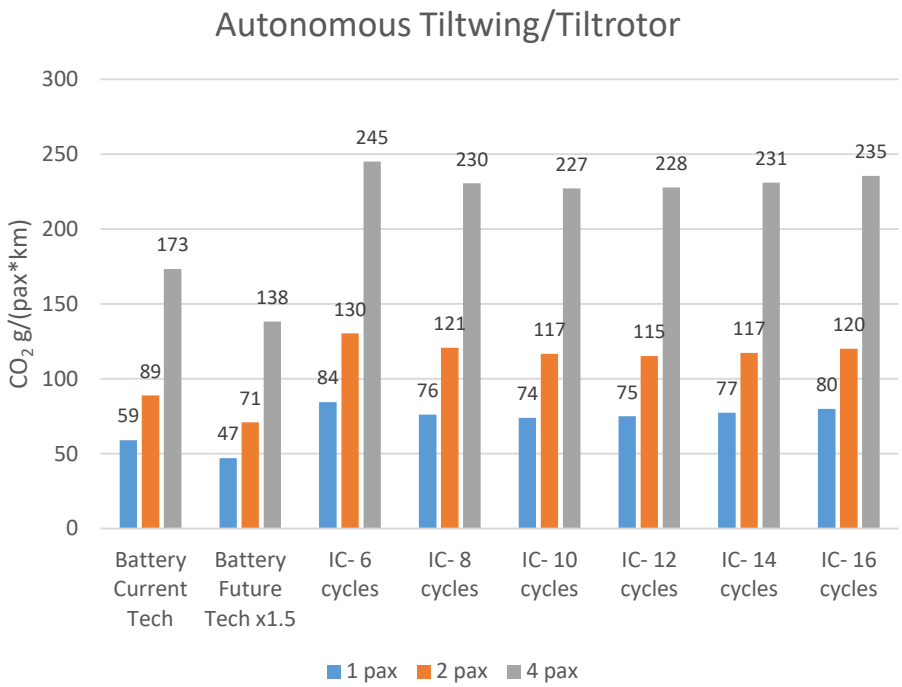

Figure 22. Autonomous tiltwing/tiltrotor vehicle CO_2 for one, two, and four passengers for different number of sizing flight cycles; batteries are both 1 cycle and the fuel is LNG.

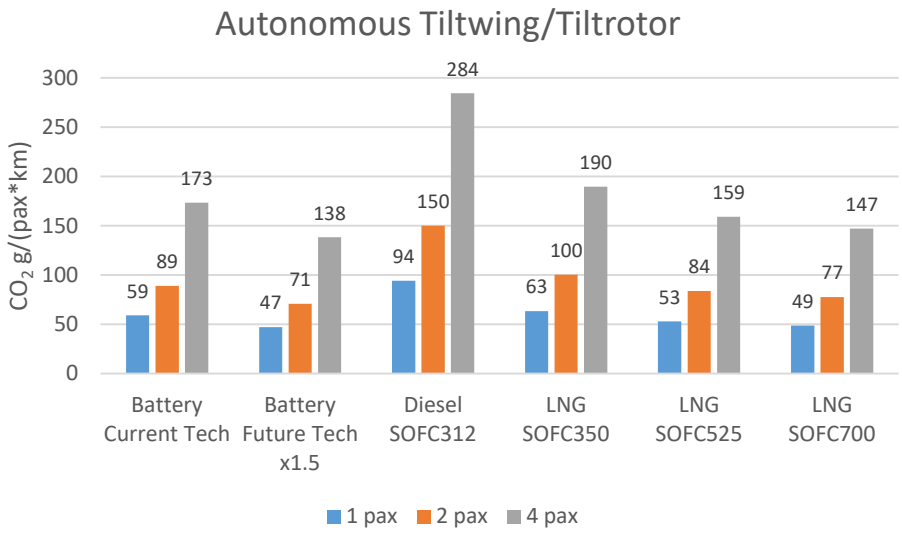

Figure 23. Autonomous tiltwing/tiltrotor vehicle CO_2 for one, two, and four passengers for different SOFC technology levels.

In Figure 23, the CO_2 g/(pax*km) is presented for different technology levels of SOFC. SOFC with LNG is shown to be immediately competitive, on a CO_2 basis, with current battery technology. Improvements to SOFC specific power result in reduced CO_2 emissions. The electric grid can also improve over time with investments in renewable energy so long-term batteries will also have a reduced carbon footprint. Renewable LNG and renewables with batteries appear to be the best routes to carbon emissions reduction.

3. Cost and Carbon Emissions Tradeoffs

Because the above results indicate that battery vehicles offer the lowest carbon emissions, but hybrid vehicles provide lower DOC, a tradeoff exists between these parameters. To help visualize these tradeoffs, the carbon emissions are plotted against the DOC, for all technologies considered, in Figure 24. The "ideal" vehicle solution would be one that minimized both CO_2 emissions and DOC, so designs that appear in the lower left portion of the figure are the most advantageous. From the figure, it is clear that the autonomous vehicles offer the potential to reduce both CO_2 emissions and DOC. Three autonomous designs on this plot are "Pareto optimal" or "non-dominated": the LNG-fueled internal combustion engine (which has the lowest DOC), the battery vehicle (which has the lowest CO_2 emissions), and the SOFC fueled with LNG (which represents a design that is "balanced" between emissions and DOC). Each of these designs has potential advantages and should, therefore, be explored in greater detail. The numbers (1, 2, and 4) next to the data points indicate the number of passengers for which the vehicle has been sized and the network operational model run to arrive at the CO_2 and DOC numbers.

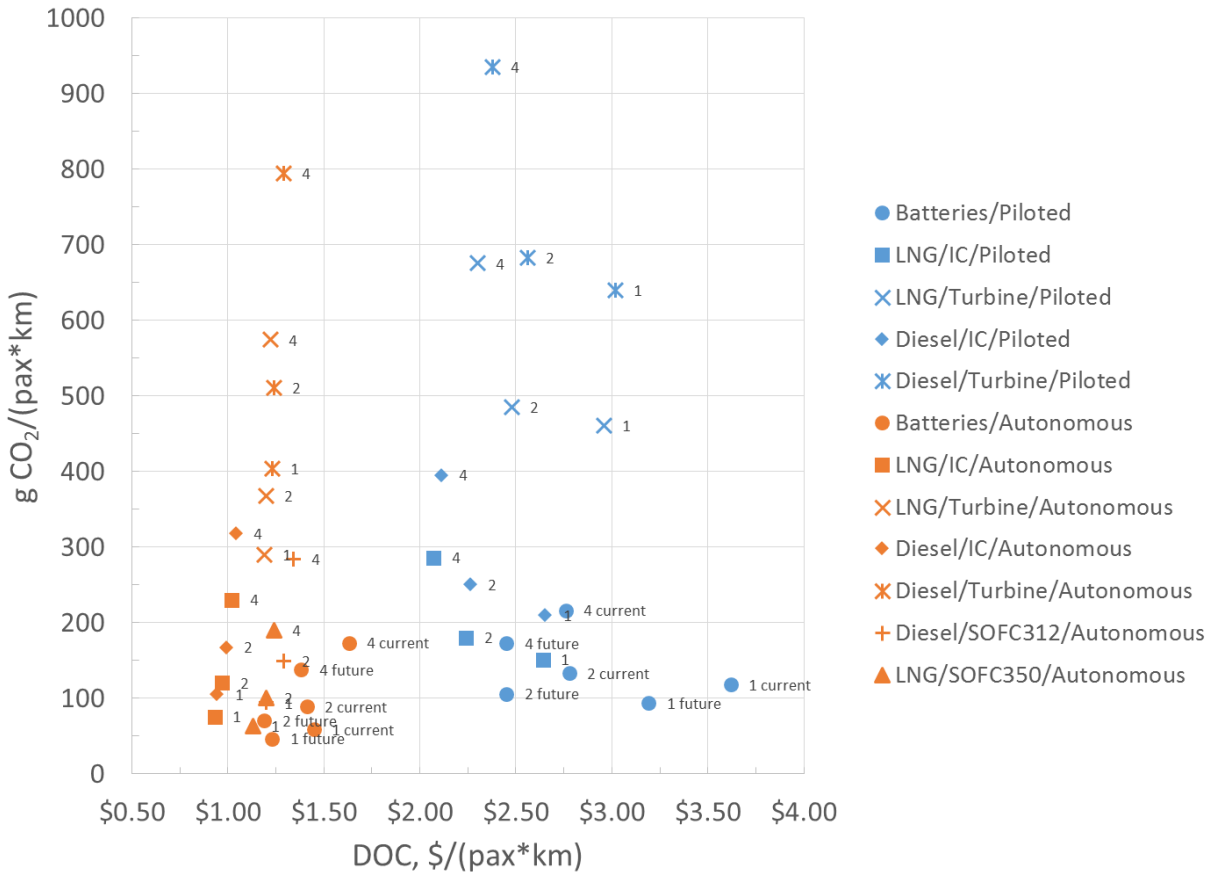

Figure 24. CO_2 emissions plotted against DOC for a variety of technologies.

V. FUTURE WORK

A. Vehicle Modeling

Preliminary estimates of vehicle characteristics needed to operate the network model in this paper were derived from simplified assumptions for the vehicle modeling. This is an initial estimate meant to capture top-level performance. Higher fidelity codes would be needed to more accurately assess the actual power loading of different vehicle types and the structural weight fraction, both of which were estimated in this work. Higher fidelity estimates could then be fed into this code to maintain fast execution of the network model.

B. Network Modeling

Network modeling is needed to make reasonable estimates of parameters such as ALF that will contribute in a significant way to the estimates of DOC and ultimately ticket price. Ticket price will play a large role in market acceptance and viability of UAM for passenger transport. The work presented here begins to evaluate the impact of various vehicle selection decisions such as vehicle type, power source, passenger count, autonomous operation, and sizing mission on DOC.

More modeling is needed to increase fidelity and to incorporate more effects in the network and cost modeling. Also, the dispatch model needs to be looked at in more depth. An optimal dispatch model would be able to handle both on-demand and scheduled flights and be optimized to work with the type or types of vehicles in the UAM network.

C. Cost Modeling

Future development of the UAM cost model necessitates an estimate for network infrastructure costs, including vertiport construction, high-voltage chargers and/or refueling stations, vertiport maintenance, ground crew salaries and training expenses, landing and parking fees, etc. Vertiport construction and charger costs are of particular interest because they will contribute significantly to the ticket price early on in the establishment of a UAM network, and may determine the ultimate feasibility of UAM operations. If the initial infrastructure costs are sufficiently high, they could prevent the establishment of a UAM network altogether.

VI. SUMMARY AND CONCLUSIONS

The exploratory modeling in this paper has demonstrated that the decisions operators make about how aircraft are dispatched around the network will have large impacts on UAM aircraft operating costs. For purely on-demand operations, it is difficult to operate multi-passenger vehicles in a way that will both maximize the number of paying passengers on board each flight and minimize the amount of time passengers must wait prior to flight departure. For operators to maximize the efficiency of their networks, strategies such as demand-based pricing and allowing or encouraging booking in advance may enable higher-efficiency networks to be realized in practice, which can lead to reduced DOCs. Additionally, the implementation of a dispatch model in this study has indicated the counterintuitive result that vehicle DOC may noticeably increase as the number of passenger seats increases when operated in a purely on-demand UAM network because of the reduced overall ALF.

Based on high-level assumptions of vehicle characteristics, which were based on the UAM literature, the modeling herein indicates that tiltrotor/tiltwing-type vehicles are likely the most appropriate for UAM aircraft regardless of propulsion system type. If battery vehicles are desired, lift-plus-cruise-type vehicles may also be appropriate, but multirotors and side-by-side helicopter configurations are not likely to result in practical vehicles. It should be noted that if a designer can find ways to make more efficient versions of the configurations studied in this paper, then these generalizations may no longer be valid.

When comparing different propulsion systems in pure-electric and hybrid-electric vehicle types, internal combustion engines provide the lowest DOC option when compared with battery-only, turbines, and SOFCs. The use of LNG as a fuel also has the potential to result in vehicles with lower costs than those using diesel or Jet-A fuel.

Battery vehicles offer the lowest carbon emissions when assuming the California grid; additionally, battery vehicles could have substantially lower emissions if the electric grid from which they are charged emits less carbon.

Near-term SOFC technologies (at 350 W/kg) with LNG fuel offer the potential to balance DOC and CO_2 emissions when compared to IC engines and batteries. Specifically, the LNG/SOFC system may provide lower DOC with only slightly higher emissions than future battery solutions on the order of 430 Wh/kg. Additionally, LNG/SOFC systems can result in lower CO_2 emissions than IC engine solutions, but slightly higher DOC.

VII. REFERENCES

[1] "Blade - The Sharpest Way to Fly," [Online]. Available: https://blade.flyblade.com/. [Accessed 20 Nov. 2018].

[2] "Urban Air Mobility Grand Challenge," NASA, [Online]. Available: https://www.nasa.gov/ uamgc. [Accessed 20 Nov. 2018].

[3] M. Moore, "Uber Elevate," in *Rotorcraft Business and Technology Summit*, 2017.

[4] Uber, "Uber Elevate | The Future of Urban Air Transport," [Online]. Available: https://www.uber.com/ info/elevate/. [Accessed 20 Nov. 2018].

[5] A. M. Stoll, E. V. Stilson, J. Bevirt, and P. P. Pei, "Conceptual Design of the Joby S2 Electric VTOL PAV," in *14th AIAA Aviation Technology, Integration, and Operations Conference*, Atlanta, GA, 2014.

[6] "Joby Aviation," [Online]. Available: http://www.jobyaviation.com/#. [Accessed 20 Nov. 2018].

[7] "Lillium | Mission," [Online]. Available: https://lilium.com/mission/. [Accessed 20 Nov. 2018].

[8] "Cora," [Online]. Available: https://cora.aero. [Accessed 20 Nov. 2018].

[9] N. K. Borer, M. D. Patterson, J. K. Viken, M. D. Moore, S. Clarke, M. E. Redifer, R. J. Christie, A. M. Stoll, A. Dubois, J. Bevirt, A. R. Gibson, T. J. Foster, and P. G. Osterkamp, "Design and Performance of the NASA SCEPTOR Distributed Electric Propulsion Flight Demonstrator," in *16th AIAA Aviation Technology, Integration, and Operations Conference, AIAA Aviation*, Washington D.C., 2016.

[10] A. M. Stoll, J. Bevirt, M. D. Moore, W. J. Fredericks, and N. K. Borer, "Drag Reduction Through Distributed Electric Propulsion," in *14th AIAA Aviation Technology, Integration, and Operations Conference*, Atlanta, GA, 2014.

[11] J. C. Patterson and S. G. Flechner, "Exploratory Wind-Tunnel Investigation of a Wingtip-Mounted Vortex Turbine for Vortex Energy Recovery," NASA Technical Paper 2468, June 1985.

[12] L. R. Miranda and J. E. Brennan, "Aerodynamic Effects of Wingtip-Mounted Propellers and Turbines," in *4th Applied Aerodynamics Conference*, San Diego, CA, 1986.

[13] W. J. Fredericks, M. D. Moore, and R. C. Busan, "Benefits of Hybrid-Electric Propulsion to Achieve 4x Cruise Efficiency for a VTOL UAV," in *2013 International Powered Lift Conference*, Los Angeles, CA, 2013.

[14] W. J. Fredericks, D. D. North, M. A. Agate, and Z. R. Johns, "NASA GL-10 Tilt-Wing VTOL UAS Flight Validation Experiments," in *AIAA Aviation*, Dallas, TX, 2015.

[15] A. Stoll, "Analysis and Full Scale Testing of the Joby S4 Propulsion System," in *Transformative Vertical Flight Workshop*, 2015.

[16] L. W. Kohlman and M. D. Patterson, "System-Level Urban Air Mobility Transportation Modeling and Determination of Energy-Related Constraints," in *AIAA Aviation*, Atlanta, GA, 2018.

[17] N. K. Borer, S. C. Geuther, B. L. Litherland, and L. W. Kohlman, "Design and Performance of a Hybrid-Electric Fuel Cell Flight Demonstration Concept," in *2018 Aviation Technology, Integration, and Operations Conference*, Atlanta, GA, 2018.

[18] M. D. Patterson, K. R. Antcliff, and L. W. Kohlman, "An Exploration of Urban Air Mobility Mission Requirements," in *AHS International 74th Annual Forum & Technology Display*, Phoenix, AZ, 2018.

[19] R. McDonald and B. German, "eVTOL Stored Energy Overview," 2017. [Online]. Available: https://uber.app.box.com/s/jy1y4gx54fb9qypxbzm78z34ax1clez5.

[20] C. Silva, W. R. Johnson, E. Solis, M. D. Patterson, and K. R. Antcliff, "VTOL Urban Air Mobility Concept Vehicles for Technology Development," in *2018 Aviation Technology, Integration, and Operations Conference*, Atlanta, GA, 2018.

[21] Google, "My Maps," [Online]. Available: https://www.google.com/mymaps. [Accessed 20 Nov. 2018].

[22] M. Daskilewicz, B. German, M. Warren, L. A. Garrow, S.-S. Boddupalli, and T. H. Douthat, "Progress in Vertiport Placement and Estimating Aircraft Range Requirements for eVTOL Daily Commuting," in *2018 Aviation Technology, Integration, and Operations Conference*, Atlanta, GA, 2018.

[23] Booz Allen Hamilton, *Detailed Project Discussion - Air Taxi*, 2018.

[24] J. Holden and N. Goel, *Fast-Forwarding to a Future of On-Demand Urban Air Transportation*, San Francisco, CA, USA: Uber, 2017.

[25] Alternative Fuels Data Center, "Fuel Prices," [Online]. Available: https:// www.afdc.energy.gov/fuels/ prices.html. [Accessed 27 Nov. 2017].

[26] D. P. Raymer, Aircraft Design: A Conceptual Approach, Washington D.C.: AIAA, 1989.